Biogeosciences Discuss., 12, 16359–16396, 2015
www.biogeosciences-discuss.net/12/16359/2015/
doi:10.5194/bgd-12-16359-2015

Biogeosciences Discussions
Open Access

Water mass characteristics and their temporal changes in a biological hotspot in the southern Chukchi Sea

S. Nishino[1], T. Kikuchi[1], A. Fujiwara[1], T. Hirawake[2], and M. Aoyama[3,4]

[1]Institute of Arctic Climate and Environment Research, Japan Agency for Marine-Earth Science and Technology, Yokosuka, Japan
[2]Faculty of Fisheries Sciences, Hokkaido University, Hakodate, Japan
[3]Research and Development Center for Global Change, Japan Agency for Marine-Earth Science and Technology, Yokosuka, Japan
[4]Institute of Environmental Radioactivity, Fukushima University, Fukushima, Japan

Received: 23 August 2015 – Accepted: 10 September 2015 – Published: 6 October 2015

Correspondence to: S. Nishino (nishinos@jamstec.go.jp)

Published by Copernicus Publications on behalf of the European Geosciences Union.

Abstract

We analysed mooring and ship-based hydrographic and biogeochemical data obtained from a Hope Valley biological hotspot in the southern Chukchi Sea. The moorings were deployed from 16 July 2012 to 19 July 2014, and data were captured during spring and fall blooms with high chlorophyll *a* concentrations. Turbidity increased and dissolved oxygen decreased in the bottom water at the mooring site before the fall bloom, suggesting an accumulation of particulate organic matter and its decomposition (nutrient regeneration) at the bottom. This event may have been a trigger for the fall bloom at this site. The bloom was maintained for 1 month in 2012 and for 2 months in 2013. The maintenance mechanism for the fall bloom was also studied by hydrographic and biogeochemical surveys in late summer to fall 2012 and 2013. Nutrient-rich water from the Bering Sea supplied nutrients to Hope Valley, although a reduction in nutrients may have occurred in 2012 by mixing of lower-nutrient water that would have remained on the Chukchi Sea shelf during the spring and fall blooms. In addition, nutrient regeneration at the bottom of Hope Valley could have increased nutrient concentrations and explained 60 % of its nutrient content in fall 2012. The high nutrient content with the dome-like structure of the bottom water may have maintained the high primary productivity at this site during the fall bloom. Primary productivity was 0.3 in September 2012 and 1.6 g C m^{-2} d^{-1} in September 2013. The lower productivity in 2012 was related to strong stratification caused by the high fraction of surface sea ice meltwater.

1 Introduction

The southern Chukchi Sea is one of the most biologically productive regions of the world's oceans because of nutrients supplied by northward flow of Pacific-originating water advected over the shelves from the northern Bering Sea into the Arctic Ocean (McRoy, 1993; Springer and McRoy, 1993; Hunt et al., 2013). Due to high primary productivity, a large quantity of organic matter descends to the sea floor as potential

BGD
12, 16359–16396, 2015

food for benthic communities, resulting in high benthic biomass (Grebmeier et al., 1988, 2006, 2015; Grebmeier, 2012). Consequently, large benthic feeders at high trophic levels, such as grey whales and walruses, also congregate there (Feder et al., 2005). Such a region of high biological activity is called a biological hotspot.

The Arctic has rapidly lost its summer sea ice cover over recent decades (Stroeve et al., 2007; Comiso et al., 2008; Kwok et al., 2009), which may significantly change ocean conditions and marine biological activities. However, the effects of extreme ice retreats and delayed sea ice formation in late autumn on primary production are uncertain in the Pacific Arctic including the Chukchi Sea, whereas clear changes have occurred in the ranges of zooplankton, benthic organisms, and fish species in summer, as well as through loss of sea ice as habitat and platforms for marine mammals (Grebmeier et al., 2010, 2015; Grebmeier, 2012). Primary productivity in the Arctic has increased in recent years, as estimated using satellite data, due to an accelerated extension of the open water area and a longer ice-free season (e.g. Arrigo et al., 2008; Pabi et al., 2008). In contrast, seasonal field measurements in the Chukchi Sea during the ice-free season in summer/fall indicate a substantial decrease in recent primary productivity compared to estimates in the 1980s (Lee et al., 2007, 2013). One of the reasons for the recent low primary productivity obtained from in situ measurements may be the large annual variation related to spatial and temporal changes in biogeochemical processes (Lee et al., 2007). Therefore, long-term monitoring using moorings with chemical and biological sensors is necessary along with ship-based hydrographic and biogeochemical surveys to better understand the responses of marine ecosystem to ongoing environmental changes in the Chukchi Sea. The southern Chukchi Sea is a suitable location for such long-term monitoring because the site is one of the most biologically productive regions and thus is in a state of significant transition, with not only environmental but also potentially economic and social consequences.

The recent loss of Arctic sea ice may also induce a second bloom in fall (fall bloom) because the delayed freeze-up and increased exposure of the sea surface to wind stress causes significant wind-driven vertical mixing and upward supply of nutrients,

BGD
12, 16359–16396, 2015

resulting in increased phytoplankton biomass. Ardyna et al. (2014) used satellite data to show that the frequency and area of fall blooms have increased recently throughout the Arctic. Nishino et al. (2015) reported fall bloom during strong wind events in the northern Chukchi Sea based on observational evidence. The increase in biomass during fall bloom could accompany changes in phyto- and zooplankton communities and may impact higher trophic levels in the ecosystem (Yokoi et al., 2015; Matsuno et al., 2015). However, the fate of the fall bloom (e.g. when it begins, the trigger, how long it continues, and the mechanism maintaining it) is unclear. Seasonal monitoring of phytoplankton biomass using water mass characteristics may provide answers to such questions.

Here, we analysed mooring and ship-based data obtained from a biological hotspot in the southern Chukchi Sea to understand the water mass characteristics (and temporal changes thereof) that influence phytoplankton biomass and productivity. Mooring data, including temperature (T), salinity (S), dissolved oxygen (DO), chlorophyll *a* (Chl *a*), and turbidity near the bottom of the biological hotspot in the southern Chukchi Sea were collected from July 2012 to July 2014 for the first time. The data were used to examine changes in water mass characteristics and phytoplankton biomass associated with spring and fall blooms in this biological hotspot. Hydrographic and biogeochemical surveys (conductivity-temperature-depth [CTD] and water sampling) were conducted across the biological hotspot during late summer to fall 2012 and 2013. We focused on the biogeochemical parameters DO, Chl *a*, turbidity, and nutrients to study the biogeochemical processes that maintain the biological hotspot until late summer and fall, and their differences between the 2 years. The effect of sea ice meltwater on primary productivity is also discussed in association with stratification of the water column.

BGD
12, 16359–16396, 2015

2 Data and methods

2.1 Mooring data

We deployed and recovered three temporally sequenced moorings (named SCH-12, SCH-12-2, and SCH-13; Table 1) from 16 July 2012 to 19 July 2014 to acquire T, S, DO, Chl *a*, and turbidity time-series near the bottom of a biological hotspot located in Hope Valley of the southern Chukchi Sea (Fig. 1). A MicroCAT C-T Recorder, SBE 37-SM (Sea-Bird Electronics, Bellevue, WA, USA) was used to acquire the T and S data. Maximum drift in the sensors over 1 year were 0.002 °C for temperature and 0.01 for salinity in pre- and post-calibration comparisons. The AROW-USB phosphorescent DO sensor was used (JFE Advantech Co., Ltd., Kobe, Japan). The sensor was calibrated using oxygen-saturated and anoxic water to determine the linear relationship between them with ±2 % accuracy. Fluorescence and backscatter were measured to obtain the Chl *a* and turbidity data, respectively, using ACLW-USB sensors (JFE Advantech). Chl *a* nonlinearity between 0 and 200 mg m^{-3} was ±1 %. The turbidity sensor was calibrated by the manufacturer using formazin standard solutions, and the results were expressed in formazin turbidity units (FTUs). Accuracy of the turbidity sensor was ±0.3 FTU or ±2 %. The data were recorded every hour and were smoothed using a running 24 h mean after removing spike noise. Because the DO value obtained on 1 September 2013 from the third mooring (SCH-13) was much higher than that from the water sample collected at the nearest location and time to the mooring data acquisition, we subtracted the excess value of 69 µmol kg^{-1} from the SCH-13 mooring DO data collected from 20 July 2013 to 19 July 2014.

To analyse the mooring data, we used the definitions of water masses from previous studies. The bottom waters in the Chukchi Sea that originate from the Pacific Ocean in summer and winter are characterised by T and S. In summer, they can be classified into three water masses: Anadyr Water ($S > 32.5$, $T = -1.0$–1.5 °C) in the west, Bering Shelf Water ($S = 31.8$–32.5, $T = 0$–4 °C) in the centre, and Alaskan Coastal Water (ACW; $S < 31.8$, $T > 4$ °C) near the Alaskan coast (Coachman et al., 1975; Coach-

BGD
12, 16359–16396, 2015

man, 1987; Grebmeier et al., 1988). As the Anadyr and Bering Shelf Waters are usually not distinct in the Chukchi Sea, the combined water mass is called the Bering Shelf-Anadyr Water (BSAW). In winter, the water mass called Bering Winter Water (BWW; S = 32.4–34.0 with near freezing temperature) occupies the Chukchi Sea (Coachman and Barnes, 1961; Kinney et al., 1970).

2.2 Ship-based data

Ship-based hydrographic and biogeochemical surveys were conducted in the Chukchi Sea and Canada Basin from 13 September to 4 October 2012 and from 31 August to 4 October 2013 on board the R/V *Mirai* of the Japan Agency for Marine-Earth Science and Technology, JAMSTEC (Fig. 1). Detailed descriptions of the 2012 and 2013 R/V *Mirai* cruises, including the above-mentioned moorings, are provided in the cruise reports (Kikuchi 2012 and Nishino 2013, respectively), and the data will be open to the public via the JAMSTEC website (http://www.godac.jamstec.go.jp/cruisedata/mirai/e/index.html). We also used data obtained from cruises of the R/V Mirai in 2004, 2008, and 2010 to compare to the data from 2012 and 2013, which were downloaded from the JAMSTEC website. The R/V *Mirai* survey periods for the area north of the Bering Strait in each year are listed in Table 2.

A CTD (SBE9plus; Sea-Bird Electronics) and a carousel water-sampling system with 36 Niskin bottles (12 L) were used to collect data. In addition, DO, light transmission, fluorescence, and photosynthetically active radiation sensors were attached to the CTD system. Seawater samples were collected to measures S, DO, total alkalinity, nutrients (nitrate, nitrite, phosphate, silicate, and ammonium), Chl *a*, primary productivity, and other chemical and biological parameters.

Bottle S samples were analysed following the Global Ocean Ship-based Hydrographic Investigations Program (GO-SHIP) Repeat Hydrography Manual using a Guideline AUTOSAL salinometer and International Association for the Physical Sciences of the Oceans standard seawater as reference material (Kawano, 2010). Precision values of the salinity measurements in 2012 and 2013 were 0.0060 and 0.0068,

BGD
12, 16359–16396, 2015

respectively, for shallow-water samples (≤ 200 m), and 0.0003 and 0.0002, respectively, for deep-water samples (> 200 m).

DO in the samples was measured by Winkler titration following World Ocean Circulation Experiment Hydrographic Program operations and methods (Dickson, 1996). Precision values for the 2012 and 2013 DO measurements were both 0.12 µmol kg^{-1}.

Total alkalinity in the samples was measured using a spectrophotometric system and the scheme reported by Yao and Byrne (1998). The total alkalinity values were calibrated against certified reference material provided by Dr. Dickson (Scripps Institute of Oceanography, La Jolla, CA, USA). The precision for the 2012 and 2013 total alkalinity measurements was 0.57 and 0.80 µmol kg^{-1}, respectively.

Nutrient samples were analysed according to the GO-SHIP Repeat Hydrography Manual (Hydes et al., 2010) using reference materials for nutrients in seawater (Aoyama and Hydes, 2010; Sato et al., 2010). The 2012 and 2013 precision values, expressed as coefficients of variation (CVs), were 0.12 and 0.11 % for nitrate, 0.21 and 0.19 % for nitrite, 0.19 and 0.11 % for phosphate, 0.11 and 0.16 % for silicate, and 0.34 and 0.30 %, for ammonium, respectively.

Chl *a* was measured in seawater samples using a fluorometric non-acidification method (Welschmeyer, 1994) and a Turner Design fluorometer (10-AU-005; Sunnyvale, CA, USA). The precision of the 2013 Chl *a* measurements (CV) was 5.3 %. Precision was not estimated in 2012 because multiple samples were not available for the estimate.

Primary phytoplankton productivity was determined using the stable ^{13}C isotope method (Hama et al., 1983). We sampled seawater from seven optical depths at 100, 38, 14, 7, 4, 1, and 0.6 % of surface irradiance. The seawater samples were inoculated with a 200 µM labelled carbon substrate ($NaH^{13}CO_3$) that represented ~ 10 % enrichment of the total inorganic carbon in ambient water. The samples were placed in an incubator for 24 h. Incubator temperature was maintained with running water from the sea surface. After incubation, the water samples were filtered through glass fibre filters (Whatman GF/F, 25 mm in diameter; Maidstone, UK) that had been pre-combusted at

BGD
12, 16359–16396, 2015

450 °C for 4 h. The ^{13}C measurements were performed onboard using a stable-isotope analyser (ANCA-SL; SerCon Ltd., Gateway, Crewe, UK). The 2012 and 2013 primary productivity precision values (CVs) were 6.5 and 7.2 %, respectively.

We used the fraction of sea ice meltwater (f_{SIM}) calculated from the relationship between potential alkalinity (total alkalinity + nitrate – ammonium) and salinity for the water mass analysis, based on Yamamoto-Kawai et al. (2009). They assumed that each seawater sample is a mixture of three end-members, such as sea ice meltwater (SIM), meteoric water (MW; river runoff + precipitation), and a saline end-member (SE). The fraction of each end-member component was estimated using the following mass balance equations:

$$f_{SIM} + f_{MW} + f_{SE} = 1, \quad (1)$$

$$f_{SIM}S_{SIM} + f_{MW}S_{MW} + f_{SE}S_{SE} = S, \quad (2)$$

$$f_{SIM}PA_{SIM} + f_{MW}PA_{MW} + f_{SE}PA_{SE} = PA \quad (3)$$

where S and PA are observed salinity and potential alkalinity of seawater, respectively, and f, S, and PA with subscripts are the fraction, salinity, and potential alkalinity, respectively, of the three SIM, MW, and SE end-members. All end-member values are listed in Table 3. This calculation was not applied to water > 4 °C, as it was largely influenced by ACW, because the end-member ACW values differed from the saline end-member values in Table 3. The fraction of sea ice meltwater, f_{SIM}, increases when seawater is influenced by sea ice melt in summer and decreases when seawater is influenced by the formation of sea ice in winter. A negative f_{SIM} implies formation of sea ice, which removes freshwater from and ejects brine into seawater, and is dominant over sea ice melt.

BGD
12, 16359–16396, 2015

3 Results

3.1 Mooring data

3.1.1 *T* and *S*

As described in Sect. 2.1, the bottom waters in the Chukchi Sea are classified into ACW, BSAW, and BWW. The *T* and *S* characteristics from the mooring data (Fig. 2a) indicate a seasonal change in water masses similar to BSAW and BWW. The BSAW occupied the bottom of the mooring site until November 2012, but it was warmer and fresher during July-October 2013 compared with 2012. The BWW was present during winter from January to May 2013 and from February to April 2014.

3.1.2 DO and turbidity

DO concentration (blue line in Fig. 2b) seemed to vary in response to the change in water masses. The BWW has high DO concentrations ($> 300\,\mu mol\,kg^{-1}$) because the water undergoes cooling and convection in winter with oxygen supplied from the atmosphere. In contrast, there is a wide range of DO concentrations in BSAW. DO concentration was high ($\sim 300\,\mu mol\,kg^{-1}$) in the beginning when the BSAW occupied the mooring site in July. Then it decreased sharply over time and had minimum values ($\sim 100\,\mu mol\,kg^{-1}$) between September and November 2012 and between August and October 2013. During these times of each year, turbidity was maximum (10–15 FTU) in an annual cycle (red line in Fig. 2b). The decrease in DO concentration and the increase in turbidity were probably related to biogeochemical processes, i.e. the deposition of particles at the bottom and decomposition of organic matter transported with the particles. This point will be discussed in Sect. 4.1.

BGD
12, 16359–16396, 2015

3.1.3 Chl *a*

The Chl *a* mooring data captured phytoplankton blooms, as indicated by high Chl *a* concentrations in spring to early summer and autumn (Fig. 2c). Chl *a* concentration increased sharply in May, when sea ice still remained in the area, and the high concentration continued until July, suggesting a spring bloom including a bloom of ice algae. The DO concentration (blue line in Fig. 2b) at the onset of the spring bloom in May increased with the increase in Chl *a*. These DO and Chl *a* increases are consistent with the oxygen production accompanying phytoplankton photosynthetic activity. Relatively high Chl *a* concentrations ($>1\,mg\,m^{-3}$) were found in September–October 2012 and August–October 2013, although the concentration was much lower than that during the spring bloom. The high concentrations during these periods probably reflected fall blooms. A time series of the turbidity (red line in Fig. 2b) data showed two peaks in accordance with annual variation in Chl *a* concentration, i.e. high turbidity in spring to early summer and autumn. However, turbidity was higher in autumn than in spring to early summer, despite lower Chl *a* concentrations in autumn. The high turbidity in autumn suggests that the turbid water contained not only phytoplankton but also other biogenic and lithogenic particles.

3.2 Ship-based data

3.2.1 Chl *a* and primary productivity

The hydrographic and biogeochemical surveys were conducted in the Chukchi Sea and the Canada Basin during September to early October 2012 and 2013, when the fall blooms were characterised by high Chl *a* and turbidity with low DO concentrations. The spatial distribution of Chl *a* integrated over the water column in 2012 (Fig. 3a) showed that the quantity of Chl *a* was relatively high in the Bering Strait, Hope Valley, and Barrow Canyon, where primary productivity in the water column was also high compared to that in the central Chukchi Sea and the Canada Basin in 2012 (Fig. 3b).

BGD
12, 16359–16396, 2015

The quantity of Chl *a* in the water column in 2013 was higher everywhere compared to 2012, and the highest quantity was detected in Hope Valley (Fig. 4a). Similarly, primary productivity integrated over the water column was higher in 2013 throughout the entire study area (Fig. 4b), and the value was highest in Hope Valley, approximately five times higher than that in 2012. Despite being downstream from nutrient-rich water from the Bering Sea, the algal biomass and primary productivity in Hope Valley were comparable to or higher than those in the Bering Strait during both years. The increases in algal biomass and primary productivity from 2012 to 2013 would have been related to a change in water stratification, which is described in detail in Sect. 3.2.3.

3.2.2 Hotspot sections in 2012

A hydrographic section was obtained from the Bering Strait to the shelf slope of the Chukchi Sea along 168°45′ W across the biological hotspot of the southern Chukchi Sea at ~ 68° N on 13–17 September 2012 (Fig. 5). We found a dome-like structure of bottom water characterised by an uplifted isohaline (isopycnal) surface at ~ 68° N with lower T and higher S (Fig. 5a), lower light transmission (Fig. 5b), and lower DO (Fig. 5c) than those of the surroundings.

We calculated f_{SIM} to examine the influence of BWW on the bottom water (T = ~ −0.4 °C, S = ~ 33.2) in the dome-like structure that was identified as BSAW. f_{SIM} had its minimum value north of 72° N at depths > 30 m above the Chukchi shelf slope (Fig. 5d). The negative f_{SIM} value means that the water was associated with brine rejection. The water there was characterised by near-freezing temperature and an S of ~ 33, and therefore, was identified as the BWW. The bottom water f_{SIM} at ~ 68° N was −0.05, smaller than that of the surrounding water (f_{SIM} ~ 0), suggesting that the BSAW in the dome-like structure was largely influenced by the BWW.

The nitrate concentration in this water (~ 7 µmol kg^{-1}) was lower than that of the Bering Strait (~ 20 µmol kg^{-1}; Fig. 5e). In contrast, the ammonium concentration was the highest in this bottom water (~ 12 µmol kg^{-1}; Fig. 5f). The ammonium concentration (~ 12 µmol kg^{-1}) reached 60 % of the total inorganic nitrogen (TIN = nitrate + nitrite +

BGD
12, 16359–16396, 2015

ammonium) concentration (~ 20 µmol kg^{-1}) in this bottom water, and it was comparable to that in the Bering Strait. Other nutrients in this bottom water, i.e. phosphate and silicate, were also comparable to those in the Bering Strait.

We revisited the biological hotspot in the southern Chukchi Sea and conducted hydrographic and biogeochemical surveys on 3–4 October 2012 (Fig. 6). Similar to the previous survey in mid September, a dome-like structure of bottom water was found at ~ 68° N with lower T and higher S (Fig. 6a), lower light transmission (Fig. 6b), and lower DO (Fig. 6c) than those of the surrounding water. However, bottom water T was higher (−0.4 °C vs. ~ 0 °C), light transmission was lower (30 % vs. 12 %), and DO was lower (130 vs. 110 µmol kg^{-1}) than the values from the previous survey. Although the negative f_{SIM} value (~ −0.03) suggests the influence of the BWW (Fig. 6d), its contribution decreased because both T and f_{SIM} increased slightly from mid September to early October. In general, light transmission and DO are higher in the BWW than in the BSAW because of the absence of particle inputs (less turbidity) and convection due to oxygen input during winter (Fig. 2b). Therefore, the decreases in light transmission and DO from mid September to early October were consistent with the decrease in the contribution of BWW to this bottom water. These changes in water properties were found in the mooring data when fluctuations of several days to a few weeks were detected, but the magnitudes of the fluctuations were smaller than the seasonal and significant yearly variation (Fig. 2). Therefore, the ship-based data represented the observed season and year.

The nitrate concentration in this water increased from 7 µmol kg^{-1} in mid September to 16 µmol kg^{-1} in early October (Fig. 6e). This may have been related to the changes in water composition described above and/or oxidation of ammonium (nitrification). The ammonium concentration remained high (~ 12 µmol kg^{-1}) in early October (Fig. 6f). The high ammonium level at this time suggests that ammonium production occurred at the bottom of the dome-like structure from mid-September to early October. This ammonium production contributed to an increase in the TIN concentration (28 µmol kg^{-1}) of the bottom water in early October 2012 in the biological hotspot of the southern

BGD
12, 16359–16396, 2015

Chukchi Sea, which became larger than the values in the previous survey, and in the Bering Strait, located upstream of the nutrient-rich BSAW.

3.2.3 Hotspot sections in 2013

We conducted hydrographic and biogeochemical surveys from the Bering Strait to the shelf slope of the Chukchi Sea along 168°45′ W from 27 September to 4 October 2013 (Fig. 7). Although we again found a dome-like structure with higher S than the surroundings, T was similar to the surroundings (Fig. 7a) and higher than that in 2012 (Figs. 5a and 6a). Light transmission was extremely low (Fig. 7b), whereas DO was almost the same as the surroundings (Fig. 7c) and higher than that in 2012 (Figs. 5c and 6c). The f_{SIM} was nearly zero, suggesting no contribution by the BWW (Fig. 7d). That is, the BSAW had likely spread from the Bering Strait to the southern Chukchi Sea around 68° N without mixing with the BWW. This finding is consistent with the higher T (Fig. 7a) in that water than in 2012 (Figs. 5a and 6a). The nitrate distribution showed a chimney of higher nitrate concentration at ∼ 68° N than the surroundings (Fig. 7e), and was higher than that in 2012 (Figs. 5e and 6e). In contrast, the ammonium concentration was ∼ 3 µmol kg^{-1} (Fig. 7f) and was markedly lower than that in 2012 (Figs. 5f and 6f).

Surface stratification in the southern Chukchi Sea was weaker in 2013 than in 2012 due to the decrease in the surface layer f_{SIM} (compare Figs. 5d, 6d, and 7d). As a result, vertical mixing that occurred in 2013 easily lifted up the bottom water to the surface, which was observed as low light transmission in surface water at ∼ 68° N, which seemed to be derived from the bottom (Fig. 7b). Vertical mixing could also have increased the DO of the bottom water there, as detected in the mooring data from the end of August 2013 (Fig. 2b) and from the ship-based data showing higher bottom water DO in 2013 than that in 2012 (compare Figs. 5c, 6c, and 7c). Thus, the weak stratification in the southern Chukchi Sea enhanced vertical mixing to supply nutrients to the surface layer, as observed in the nitrate profile (Fig. 7e), resulting in the higher algal biomass and primary productivity in 2013 than in 2012 (compare Figs. 3 and 4).

BGD
12, 16359–16396, 2015

3.2.4 Hotspot sections in the previous surveys

Hydrographic and biogeochemical surveys were also conducted in the Chukchi Sea along 168°45′ W in late summer to fall 2004, 2008, and 2010 (Table 2). The vertical sections of the water properties were all similar to those in 2013 as described below; hence, we show the mean features of the vertical sections during these years (Fig. 8). The dome-like structure of the Hope Valley (~ 68° N) bottom water was characterised by an uplifted isohaline (isopycnal) surface with lower T and higher S (Fig. 8a), lower light transmission (Fig. 8b), and lower DO (Fig. 8c) than those of the surroundings. Although the T, S, and DO characteristics were not as significant as those in 2012, the dome-like structure was a robust feature of the biological hotspot in the southern Chukchi Sea.

As in 2013, the bottom water f_{SIM} value was nearly zero (Fig. 8d), suggesting that the small contribution of the BWW did not change the characteristics of the BSAW significantly on its way from the Bering Strait to Hope Valley. As a result, the T of the bottom water in Hope Valley did not decrease significantly from that in the Bering Strait (Fig. 8a). Similarly, nitrate concentration at the bottom of Hope Valley was slightly lower from that in the Bering Strait but remained higher than that of the surroundings (Fig. 8e). In comparison, the ammonium concentration at Hope Valley was the highest (Fig. 8f), suggesting a large amount of ammonium production there.

4 Discussion

4.1 Fall bloom and biogeochemical processes

The mooring data obtained with sensors installed near the bottom in the biological hotspot of the southern Chukchi Sea revealed two novel results regarding the annual cycle of water characteristics related to biogeochemical processes. A large decrease in bottom water DO occurred just before the fall bloom but not at the spring bloom (Fig. 2b

BGD
12, 16359–16396, 2015

and c). The decrease in DO was accompanied by an increase in bottom water turbidity, and DO (turbidity) had minimum (maximum) values during the fall bloom. Yamada et al. (2015) observed that the concentrations of particles and particulate organic matter (POM) are extremely high at the bottom of Hope Valley in autumn, suggesting that particles including POM accumulate at the bottom there in autumn with an increase in turbidity and decrease in oxygen used to decompose accumulated POM. One conceivable source of such particles is an upstream region of northward currents that transport the BSAW through the Bering Strait (e.g. Grebmeier, 2012; Mathis et al., 2014; Grebmeier et al., 2015). This is consistent with the finding that the surface sediment along the BSAW pathway has a high amount of total organic carbon, including a large quantity of marine organic matter (phytoplankton and marine algal detritus) available to benthic populations (Grebmeier et al., 1988, 2006). The ACW could also carry Yukon River sediments (McManus et al., 1969). However, such terrestrial inputs would be difficult for use in biological processes (Grebmeier et al., 1988, 2006). Moran et al. (2005) suggested that part of the production is exported laterally and off the Chukchi Sea shelf during the most productive season. Therefore, in addition to export production, lateral transport of organic particles is important for oxygen consumption by sediment communities, particularly during the fall bloom season.

The DO concentration at the bottom of the mooring site in the southern Chukchi Sea did not decrease significantly during the spring bloom or soon after the bloom. However, oxygen was largely consumed (in June) on the bottom south of St. Lawrence Island in the Bering Sea just after Chl *a* concentrations peaked in the water column (May–June) with a time lag of days to weeks for organic material to become part of the surface sediment (Cooper et al., 2002). In general, significant correlations are observed between spatial patterns of the standing stock of Chl *a* in the water column and the oxygen consumption of the underlying sediment community in the Bering and Chukchi Sea shelves (Grebmeier et al., 2006; Grebmeier, 2012). However, lateral transport of organic particles along northward currents of the BSAW in the southern Chukchi Sea may be important for oxygen consumption by the sediment community. The minimum

BGD
12, 16359–16396, 2015

levels of oxygen at the bottom during the fall bloom in an annual cycle would not be due to a local spring phytoplankton bloom but rather would result from POM decomposition including allochthonous organic particles that accumulate in the Hope Valley topographic depression.

The mooring data in this study further suggest that the onset of particle accumulation and POM decomposition at the bottom of Hope Valley occurred from the end of July to the beginning of August in 2012 and 2013, when turbidity increased and the DO concentration decreased with time (Fig. 2b). However, Chl *a* concentrations decreased during this period (Fig. 2c). The increase in Chl *a* toward the fall bloom started in mid-September in 2012 and in mid-August in 2013. Therefore, particle accumulation and the decomposition of POM (nutrient regeneration) may have been necessary before the onset of the fall bloom. The bloom continued for 1 month (mid-September to mid-October) in 2012 and for 2 months (mid-August to mid-October) in 2013. The fall bloom has been assumed to result from fall events, such as storms, surface cooling, and formation of sea ice (Ardyna et al., 2013, 2014). However, our data suggest that the fall bloom is triggered by the accumulation of particles and POM decomposition that begin in summer (end of July to beginning of August), at least in the Hope Valley of the southern Chukchi Sea, and that the bloom is not an event-like phenomenon, but has a time scale of months with fluctuations that may be related to the fall events.

4.2 Dome-like structure in the southern Chukchi Sea

We found a dome-like structure of dense and turbid bottom water in the biological hotspot of the southern Chukchi Sea based on hydrographic surveys during fall blooms (Figs. 5–8). The dome-like structure was associated with the Hope Valley topographic depression where dense water may converge and particles likely accumulate. The bottom water characteristics depended on the influences of the BSAW and BWW. The water in 2012, which likely originated from the BSAW, was modified by mixing with the BWW (Figs. 5d and 6d). However, the BSAW occupied the bottom of Hope Valley without any contribution by the BWW in 2013 (Fig. 7d). The large influence of the BWW

BGD
12, 16359–16396, 2015

in 2012 produced a prominent core of lower temperature and higher salinity (density) there compared to the surrounding area (Figs. 5a and 6a). However, the lack of a contribution by the BWW in 2013 resulted in a temperature and salinity similar to the surroundings (Fig. 7a).

Nutrient concentrations there were also controlled by the influences of the BSAW and BWW. In general, nutrient concentrations in the BSAW increase toward the south, in regions upstream of the flow (e.g. Springer and McRoy, 1993; Grebmeier et al., 2015), and nitrate concentration is $>20\,\mu mol\,kg^{-1}$ in the Gulf of Anadyr, where nutrient-rich Pacific waters are first advected up onto the Bering Sea shelf, which corresponds to that in the nutrient maximum layer of the upper halocline of the Arctic (e.g. Jones and Anderson, 1986; Cooper et al., 1997). Similarly, the nitrate concentration in the BWW during winter was $\sim 20\,\mu mol\,kg^{-1}$ because nutrients in the Bering and Chukchi shelves undergo little biological uptake during winter (Hansell et al., 1993; Cooper et al., 1997). However, if the BWW remains on the Chukchi shelf until the next summer/fall, nutrients are supplied to the upper layer via vertical mixing and are used for biological production (Lowry et al., 2015; Nishino et al., 2015). As a result, this remnant BWW on the Chukchi shelf may have low nutrient concentrations, as observed at 72–73° N near the shelf slope. The nitrate concentration there was $\leq 10\,\mu mol\,kg^{-1}$ in the fall of both 2012 and 2013 (Figs. 5e and 7e). Therefore, the contribution to Hope Valley bottom water due to the remnant BWW, such as in 2012, could reduce nutrient concentrations there. In fact, the nitrate concentration there, which was a mixture of the BSAW and BWW in 2012 (Fig. 5e; $\sim 7\,\mu mol\,kg^{-1}$), was lower than that of the bottom water identified as the BSAW without influence from the BWW in 2013 (Fig. 7e; $\sim 16\,\mu mol\,kg^{-1}$).

Another important process controlling nutrient concentrations was ammonium production. Except for 2013, ammonium had maximum concentrations at the bottom of Hope Valley in the southern Chukchi Sea (Fig. 8f). In addition, the lowest light transmission and oxygen concentration were found there (Fig. 8b and c, respectively); i.e. a large amount of POM accumulated at the bottom of Hope Valley and its decomposition decreased oxygen and increased ammonium concentrations as a result of

BGD
12, 16359–16396, 2015

nutrient regeneration. The decomposing POM consumed oxygen and produced ammonium, generating a linear relationship between DO and ammonium concentrations in the southern Chukchi Sea (Fig. 9). The TIN at the bottom of Hope Valley in the fall of 2012 was comparable to that in the Bering Strait, which is located upstream of the nutrient-rich BSAW flow. This high concentration ($\sim 20\,\mu mol\,kg^{-1}$) was attributed to the high concentration of ammonium ($\sim 12\,\mu mol\,kg^{-1}$), suggesting significant nutrient regeneration at the bottom, which explained 60 % of the nutrient content. The TIN there in fall 2013 was $\sim 20\,\mu mol\,kg^{-1}$ but ammonium was only $\sim 3\,\mu mol\,kg^{-1}$, which does not support the scenario that nutrient regeneration at that time was lower than in fall 2012. The weak stratification in fall 2013 may have diluted the ammonium levels via mixing with ammonium-free water in the upper layer, whereas bottom water nitrate was not diluted as much because nitrate in the upper layer was likely not depleted due to the influence of the BSAW. Therefore, it was difficult to estimate the contribution of nutrient regeneration to the nutrient content in the Hope Valley bottom water for 2013. However, nutrient regeneration may have occurred significantly even in the fall 2013 because turbid water was still present, suggesting the accumulation of POM.

POM was largely carried by the BSAW during the fall of 2012 and 2013 and accumulated in the Hope Valley topographic depression. The nutrient regeneration caused by decay of POM at this site would help increase bottom water nutrient concentrations. Furthermore, the dome-like structure lifts up the isopycnal surface, and nutrients would be supplied to the surface (euphotic zone) easier than to the surroundings. Vertical nutrient supply would be enhanced when stratification was weak, such as in 2013. For example, nitrogenous compounds are usually depleted at the sea surface where a relatively high level of ammonium ($\sim 1\,\mu mol\,kg^{-1}$) was found in fall 2013, suggesting nutrient regeneration at the bottom and vertical transport of the ammonium produced via vertical mixing (Fig. 7f). Indeed, the nutrient supply from the BSAW is important for the phytoplankton bloom during spring and early summer, as discussed by Springer and McRoy (1993). However, the combination of nutrient regeneration at the bottom and the uplifted isopycnal surface accompanied by the dome-like structure played an

BGD
12, 16359–16396, 2015

important role maintaining the high productivity of the biological hotspot in the southern Chukchi Sea at least during late summer and fall.

4.3 Stratification and primary productivity

Although Hope Valley maintained high primary productivity during late summer and fall, the magnitude was controlled by stratification of the water column. Primary productivity there was 0.3 g C m^{-2} d^{-1} in September 2012 and 1.6 g C m^{-2} d^{-1} in September 2013 (Figs. 3 and 4). The 2013 productivity was consistent with that estimated from in situ measurements during the same season from 2002 to 2004 (1.4 g C m^{-2} d^{-1}; Lee et al., 2007) and in 2007 (1.6 g C m^{-2} d^{-1}; Lee et al., 2013). The lower productivity in 2012 than in 2013 and in recent years was related to the strong stratification in 2012 caused by the high fraction of sea ice meltwater at the surface (Fig. 5d). Sea ice remained until September 2012 around Wrangel Island between the Chukchi and East Siberian Seas and may have resulted in the high fraction of sea ice meltwater at the surface of the Chukchi Sea, including the Hope Valley area.

Primary productivity in the Chukchi Sea in recent years seemed to decrease from that reported in the 1980s (Lee et al., 2007, 2013). Lee et al. (2007) hypothesised that the difference in primary productivity was associated with changes in water masses, the transport of nutrients with phytoplankton and sediments, primary productivity in the Bering Sea, and the large seasonal, annual, and geographical variation in primary productivity in the Chukchi Sea. Our results further suggest a large influence of sea ice meltwater in September 2012 on the reduction of primary productivity in the Chukchi Sea. Furthermore, data obtained in September 2009 indicated that high amounts of freshwater accumulated in the Chukchi Sea from Siberian coastal currents and negatively affected primary productivity (Yun et al., 2014). Such freshwater distributions, which control water column stratification, and thus primary productivity, are likely changed by wind- and buoyancy-forced currents on synoptic and seasonal time scales (Weingartner et al., 1999). Hence, synoptic and seasonal events could largely impact the fall bloom, and the frequency and magnitude of the bloom may not neces-

BGD
12, 16359–16396, 2015

sarily increase with a delay in fall freeze-up (longer ice-free season), as expected from satellite data (e.g. Arrigo et al., 2008; Pabi et al., 2008; Ardyna et al., 2014).

5 Summary

We analysed mooring and ship-based data obtained from a biological hotspot in the southern Chukchi Sea to understand water mass characteristics and their temporal changes, and how they influence phytoplankton biomass and productivity there. The mooring data indicated a seasonal change in water masses, i.e. the BSAW in summer/fall and BWW in winter/spring. The ship-based hydrographic and biogeochemical data suggested that the BSAW was largely modified by the BWW in fall 2012 but not during a typical fall (2004, 2008, 2010, and 2013). As a result, a prominent core of bottom water, which was characterised by lower temperature and higher salinity (density) than the surrounding water, was detected in 2012. The large influence of the BWW in 2012 would have reduced nutrient concentrations because nutrients in the BWW that had remained in the Chukchi Sea until summer/fall were probably used for the spring and fall blooms. In contrast, nutrient regeneration at the bottom increased nutrient concentrations and explained 60 % of the nutrient levels there in 2012. This high nutrient content, which was supplied by the BSAW and nutrient regeneration in the dome-like structure of the Hope Valley bottom water, maintained high primary productivity during the fall bloom. However, primary productivity was largely controlled by water column stratification characterised by the distribution of freshwater from sea ice meltwater and river water. Thus, there was large temporal and spatial variation in primary productivity and phytoplankton biomass. Therefore, long-term monitoring using moorings and chemical and biological sensors is necessary.

Although the mooring in this study was deployed only at the biological hotspot site in the southern Chukchi Sea, the data show a temporal change in phytoplankton biomass and related parameters for the first time. We observed spring and fall blooms associated with high Chl *a* concentrations. Before the fall bloom, turbidity increased and DO

BGD
12, 16359–16396, 2015

decreased, suggesting accumulation and decomposition of POM (nutrient regeneration) on the bottom. This may have been a trigger for the fall bloom at this site. The mooring data further suggest that the fall bloom had a time scale of months with fluctuations that might have been related to fall events, such as storms, surface cooling, and the formation of sea ice.

Acknowledgements. We thank the captain, officers, and crew of the R/V *Mirai*, which was operated by Global Ocean Development, Inc. We also thank the staff of Marine Works Japan, Ltd., for their skilful work aboard the ship and for data processing. This study was supported by the Green Network of Excellence Program (GRENE Program), which is funded by the Arctic Climate Change Research Project of the Ministry of Education, Culture, Sports, Science and Technology of Japan (MEXT). Maps and figures were drawn using Ocean Data View software (Schlitzer, 2015). The data used to prepare this study will be released from the JAMSTEC Data Site for Research Cruises (http://www.godac.jamstec.go.jp/cruisedata/mirai/e/index.html).

References

Aoyama, M. and Hydes, D. J.: How do we improve the comparability of nutrient measurements?, in: Comparability of Nutrients in the World's Ocean, edited by: Aoyama, M., Dickson, A. G., Hydes, D. J., Murata, A., Oh, J. R., Roose, P., and Woodward E. M. S., Mother Tank, Tsukuba, Japan, 1–10, 2010.

Ardyna, M., Babin, M., Gosselin, M., Devred, E., Bélanger, S., Matsuoka, A., and Tremblay, J.-É.: Parameterization of vertical chlorophyll *a* in the Arctic Ocean: impact of the subsurface chlorophyll maximum on regional, seasonal, and annual primary production estimates, Biogeosciences, 10, 4383–4404, doi:10.5194/bg-10-4383-2013, 2013.

Ardyna, M., Babin, M., Gosselin, M., Devred, E., Rainville, L., and Tremblay, J.-É.: Recent Arctic Ocean sea ice loss triggers novel fall phytoplankton blooms, Geophys. Res. Lett., 41, 6207–6212, doi:10.1002/2014GL061047, 2014.

Arrigo, K. R., van Dijken, G., and Pabi, S.: Impact of a shrinking Arctic ice cover on marine primary production, Geophys. Res. Lett., 35, L19603, doi:10.1029/2008GL035028, 2008.

BGD
12, 16359–16396, 2015

Coachman, L. K.: Advection and mixing on the Bering-Chukchi Shelves, Component A, Advection and mixing of coastal water on high latitude shelves, ISHTAR 1986 Progress Report, Vol. I, Inst. Mar. Sci., Univ. Alaska, Fairbanks, 1–42, 1987.
Coachman, L. K. and Barnes, C. A.: The contribution of Bering Sea water to the Arctic Ocean, Arctic, 14, 147–161, 1961.
Coachman, L. K., Aagaard, K., and Tripp, R. B.: Bering Strait: The regional physical oceanography, Univ. of Washington Press, Seattle, 172 pp., 1975.
Comiso, J. C., Parkinson, C. L., Gersten, R., and Stock, L.: Accelerated decline in the Arctic sea ice cover, Geophys. Res. Lett., 35, L01703, doi:10.1029/2007GL031972, 2008.
Cooper, L. W., Whitledge, T. E., Grebmeier, J. M., and Weingartner, T.: The nutrient, salinity, and stable oxygen isotope composition of Bering and Chukchi Seas waters in and near the Bering Strait, J. Geophys. Res., 102, 12563–12573, 1997.
Cooper, L. W., Grebmeier, J. M., Larsen, I. L., Egorov, V. G., Theodorakis, C., Kelly, H. P., and Lovvorn, J. R.: Seasonal variation in water column processes and sedimentation of organic materials in the St. Lawrence Island polynya region, Bering Sea, Mar. Ecol.-Prog. Ser., 226, 13–26, 2002.
Dickson, A. G.: Determination of dissolved oxygen in sea water by Winkler titration, in: WOCE Operations Manual, Volume 3, Section 3.1, Part 3.1.3 WHP Operations and Methods, WHP Office Report WHPO 91-1, WOCE Report No. 68/91, Nov. 1994, Revision 1, Woods Hole, Mass., 13 pp., 1996.
Feder, H., Jewett, S., and Blanchard, A.: Southeastern Chukchi Sea (Alaska) epibenthos, Polar Biol., 28, 402–421, 2005.
Grebmeier, J. M.: Shifting patterns of life in the Pacific Arctic and sub-Arctic seas, Annu. Rev. Mar. Sci., 4, 63–78, doi:10.1146/annurev-marine-120710-100926, 2012.
Grebmeier, J. M., McRoy, C. P., and Feder, H. M.: Pelagic-benthic coupling on the shelf of the northern Bering and Chukchi Seas. I. Food supply source and benthic biomass, Mar. Ecol.-Prog. Ser., 48, 57–67, 1988.
Grebmeier, J. M., Cooper, L. W., Feder, H. M., and Sirenko, B. I.: Ecosystem dynamics of the Pacific-influenced Northern Bering and Chukchi Seas in the Amerasian Arctic, Prog. Oceanogr., 71, 331–361, 2006.
Grebmeier, J. M., Moore, S. E., Overland, J. E., Frey, K. E., and Gradinger, R.: Biological response to recent Pacific Arctic sea ice retreats, EOS, 91, 161–162, 2010.

BGD
12, 16359–16396, 2015

Grebmeier, J. M., Bluhm, B. A., Cooper, L. W., Danielson, S. L., Arrigo, K. R., Blanchard, A. L., Clarke, J. T., Day, R. H., Frey, K. E., Gradinger, R. R., Kedra, M., Konar, B., Kuletz, K. J., Lee, S. H., Lovvorn, J. R., Norcross, B. L., and Okkonen, S. R.: Ecosystem characteristics and processes facilitating persistent macrobenthic biomass hotspots and associated benthivory in the Pacific Arctic, Prog. Oceanogr., 136, 92–114, doi:10.1016/j.pocean.2015.05.006, 2015.

Hama, T., Miyazaki, T., Ogawa, Y., Iwakuma, T., Takahashi, M., Otsuki, A., and Ichimura, S.: Measurement of photosynthetic production of a marine phytoplankton population using a stable ^{13}C isotope, Mar. Biol., 73, 31–36, 1983.

Hansell, D. A., Whitledge, T. E., and Goering, J. J.: Patterns of nitrate utilization and new production over the Bering-Chukchi shelf, Cont. Shelf Res., 13, 601–627, 1993.

Hunt Jr., G. L., Blanchard, A. L., Boveng, P., Dalpadado, P., Drinkwater, K. F., Eisner, L., Hopcroft, R. R., Kovacs, K. M., Norcross, B. L., Renaud, P., Reigstad, M., Renner, M., Skjoldal, H. R., Whitehouse, A., and Woodgate, R. A.: The Barents and Chukchi Seas: Comparison of two Arctic shelf ecosystems, J. Mar. Syst., 109–110, 43–68, doi:10.1016/j.jmarsys.2012.08.003, 2013.

Hydes, D. J., Aoyama, M., Aminot, A., Bakker, K., Becker, S., Coverly, S., Daniel, A., Dickson, A. G., Grosso, O., Kerouel, R., van Ooijen, J., Sato, K., Tanhua, T., Woodward, E. M. S. and Zhang, J. Z.: Determination of dissolved nutrients (N, P, Si) in seawater with high precision and inter-comparability using gas-segmented continuous flow analysers, in: The GO-SHIP Repeat Hydrography Manual: A Collection of Expert Reports and Guidelines, IOCCP Report Number 14, ICPO Publication Series Number 134, edited by: Hood, E. M., Sabine, C. L., and Sloyan, B. M., UNESCO-IOC, Paris, France, available at: www.go-ship.org/HydroMan.html (last access: 25 September 2015), 2010.

Jones, E. P. and Anderson, L. G.: On the origin of the chemical properties of the Arctic Ocean halocline, J. Geophys. Res., 91, 10759–10767, 1986.

Kawano, T.: Method for salinity (conductivity ratio) measurement, in: The GO-SHIP Repeat Hydrography Manual: A Collection of Expert Reports and Guidelines, IOCCP Report Number 14, ICPO Publication Series Number 134, edited by: Hood, E. M., Sabine, C. L., and Sloyan, B. M., UNESCO-IOC, Paris, France, available at: www.go-ship.org/HydroMan.html (last access: 25 September 2015), 2010.

Kikuchi, T.: R/V *Mirai* Cruise Report MR12-E03, JAMSTEC, Yokosuka, Japan, available at: www.godac.jamstec.go.jp/cruisedata/mirai/e/index.html (last access: 25 September 2015), 2012.

BGD
12, 16359–16396, 2015

Kinney, P., Arhelger, M. E., and Burrell, D. C.: Chemical characteristics of water masses in the American Basin of the Arctic Ocean, J. Geophys. Res., 75, 4097–4104, 1970.
Kwok, R., Cunningham, G. F., Wensnahan, M., Zwally, H. J., and Yi, D.: Thinning and volume loss of the Arctic Ocean sea ice cover: 2003–2008, J. Geophys. Res., 114, C07005, doi:10.1029/2009JC005312, 2009.
Lee, S. H., Whitledge, T. E., and Kang, S. H.: Recent carbon and nitrogen uptake rates of phytoplankton in Bering Strait and the Chukchi Sea, Cont. Shelf Res., 27, 2231–2249, doi:10.1016/j.csr.2007.05.009, 2007.
Lee, S. H., Yun, M. S., Kim, B. K., Saitoh, S. I., Kang, C. K., Kang, S. H., and Whitledge, T. E.: Latitudinal carbon productivity in the Bering and Chukchi seas during the summer in 2007, Cont. Shelf Res., 59, 28–36, doi:10.1016/j.csr.2013.04.004, 2013.
Lowry, K. E., Pickart, R. S., Mills, M. M., Brown, Z. W., vanDijken, G. L., Bates, N. R., and Arrigo, K. R.: The influence of winter water on phytoplankton blooms in the Chukchi Sea, Deep-Sea Res. Pt. II, 62, doi:10.1016/j.dsr2.2015.06.006, 2015.
Mathis, J. T., Grebmeier, J. M., Hansell, D. A., Hopcroft, R. R., Kirchman, D. L., Lee, S. H., Moran, S. B., Bates, N. R., VanLaningham, S., Cross, J. N., and Cai, W.-J.: Carbon Biogeochemistry of the Western Arctic: Primary Production, Carbon Export and the Controls on Ocean Acidification, in: The Pacific Arctic region, Ecosystem Status and Trends in a Rapidly Changing Environment, edited by: Grebmeier, J. M. and Maslowski, W., Springer, Dordrecht, Netherlands, 223–268, doi:10.1007/978-94-017-8863-2, 2014.
Matsuno, K., Yamaguchi, A., Nishino, S., Inoue, J., and Kikuchi, T.: Short-term changes in the mesozooplankton community and copepod gut pigment in the Chukchi Sea in autumn: reflections of a strong wind event, Biogeosciences, 12, 4005–4015, doi:10.5194/bg-12-4005-2015, 2015.
McManus, D. A., Kelley, J. C., and Creager, J. S.: Continental Shelf Sedimentation in an Arctic Environment, Geol. Soc. Am. Bull., 80, 1961–1984, 1969.
McRoy, C. P.: ISHTAR, the project: an overview of Inner Shelf Transfer And Recycling in the Bering and Chukchi seas, Cont. Shelf Res., 13, 473–479, 1993.
Moran, S. B., Kelly, R. P., Hagstrom, K., Smith, J. N., Grebmeier, J. M., Cooper, L. W., Cota, G. F., Walsh, J. J., Bates, N. R., Hansell, D. A., Maslowski, W., Nelson, R. P., and Mulsow, S.: Seasonal changes in POC export flux in the Chukchi Sea and implications for water column-benthic coupling in Arctic shelves, Deep-Sea Res. Pt. II, 52, 3324–3343, 2005.

BGD
12, 16359–16396, 2015

Nishino, S.: R/V *Mirai* Cruise Report MR13-06. JAMSTEC, Yokosuka, Japan, available at: www.godac.jamstec.go.jp/darwin/datatree/e (last access: 25 September 2015), 2013.
Nishino, S., Kawaguchi, Y., Inoue, J., Hirawake, T., Fujiwara, A., Futsuki, R., Onodera, J., and Aoyama, M.: Nutrient supply and biological response to wind-induced mixing, inertial motion, internal waves, and currents in the northern Chukchi Sea, J. Geophys. Res. Oceans, 120, 1975–1992, doi:10.1002/2014JC010407, 2015.
Pabi, S., van Dijken, G. L., and Arrigo, K. R.: Primary production in the Arctic Ocean, 1998–2006, J. Geophys. Res., 113, C08005, doi:10.1029/2007JC004578, 2008.
Sato, K., Aoyama, M., and Becker, S.: Reference materials for nutrients in seawater as calibration standard solution to keep comparability for several cruises in the world ocean in 2000s, in: Comparability of Nutrients in the World's Ocean, edited by: Aoyama, M., Dickson, A. G., Hydes, D. J., Murata, A., Oh, J. R., Roose, P., and Woodward E. M. S., Mother Tank, Tsukuba, Japan, 43–56, 2010.
Schlitzer, R.: Ocean Data View. Alfred Wegener Institute, Bremerhaven, Germany, available at: http://odv.awi.de (last access: 25 September 2015), 2015.
Springer, A. M. and McRoy, C. P.: The paradox of pelagic food webs in the northern Bering Sea-III. Patterns of primary productivity, Cont. Shelf Res., 13, 575–599, 1993.
Stroeve, J., Holland, M. M., Meier, W., Scambos, T., and Serreze, M.: Arctic sea ice decline: Faster than forecast, Geophys. Res. Lett., 34, L09501, doi:10.1029/2007GL029703, 2007.
Weingartner, T. J., Danielson, S., Sasaki, Y., Pavlov, V., and Kulakov, M.: The Siberian Coastal Current: A wind- and buoyancy-forced Arctic coastal current, J. Geophys. Res., 104, 29697–29713, doi:10.1029/1999JC900161, 1999.
Welschmeyer, N. A.: Fluorometric analysis of chlorophyll *a* in the presence of chlorophyll *b* and pheopigments, Limnol. Oceanogr., 39, 1985–1992, 1994.
Yamada, Y., Fukuda, H., Uchimiya, M., Motegi, C., Nishino, S., Kikuchi, T., and Nagata, T.: Localized accumulation and a shelf-basin gradient of particles in the Chukchi Sea and Canada Basin, western Arctic, J. Geophys. Res. Oceans, 120, 4638–4653, doi:10.1002/2015JC010794, 2015.
Yamamoto-Kawai, M., McLaughlin, F. A., Carmack, E. C., Nishino, S., Shimada, K., and Kurita, N.: Surface freshening of the Canada Basin, 2003–2007: River runoff versus sea ice meltwater, J. Geophys. Res., 114, C00A05, doi:10.1029/2008JC005000, 2009.
Yao, W. and Byrne, R. H.: Simplified seawater alkalinity analysis: Use of linear array spectrometers, Deep-Sea Res. Pt. I, 45, 1383–1392, 1998.

BGD
12, 16359–16396, 2015

Yokoi, N., Matsuno, K., Ichinomiya, M., Yamaguchi, A., Nishino, S., Onodera, J., Inoue, J., and Kikuchi, T.: Short-term changes in a microplankton community in the Chukchi Sea during autumn: consequences of a strong wind event, Biogeosciences Discuss., 12, 8789–8817, doi:10.5194/bgd-12-8789-2015, 2015.

Yun, M. S., Whitledge, T. E., Kong, M., and Lee, S. H.: Low primary production in the Chukchi Sea shelf, 2009, Cont. Shelf Res., 76, 1–11, doi:10.1016/j.csr.2014.01.001, 2014.

BGD
12, 16359–16396, 2015

Table 1. Mooring configurations.

Mooring	Latitude	Longitude	Bottom Depth	Sensor Depth	Parameters	Period
SCH-12	67°42.18′ N	168°50.01′ W	52 m	45 m	*T*, *S*, DO, Chl *a*, turbidity	16 July 2012–2 October 2012
SCH-12-2	68°02.00′ N	168°50.03′ W	59 m	52 m	*T*, *S*, DO, Chl *a*, turbidity	3 October 2012–20 July 2013
SCH-13	68°02.00′ N	168°50.03′ W	60 m	53 m	*T*, *S*, DO, Chl *a*, turbidity	20 July 2013–19 July 2014

Notes: *T*, *S*, DO, and chl *a* denote temperature, salinity, dissolved oxygen, and chlorophyll *a*, respectively.

BGD
12, 16359–16396, 2015

Table 2. R/V *Mirai* survey periods.

Year	Period
2004	3 September–9 October
2008	28 August–6 October
2010	4 September–13 October
2012	13 September–4 October
2013	31 August–4 October

BGD
12, 16359–16396, 2015

Table 3. End-member values used in this study.

	Salinity	Potential Alkalinity ($\mu mol\,kg^{-1}$)
SIM (sea ice meltwater)	4	263
MW (meteoric water = river runoff + precipitation)	0	793
SE (saline end-member)	32.5	2223

BGD
12, 16359–16396, 2015

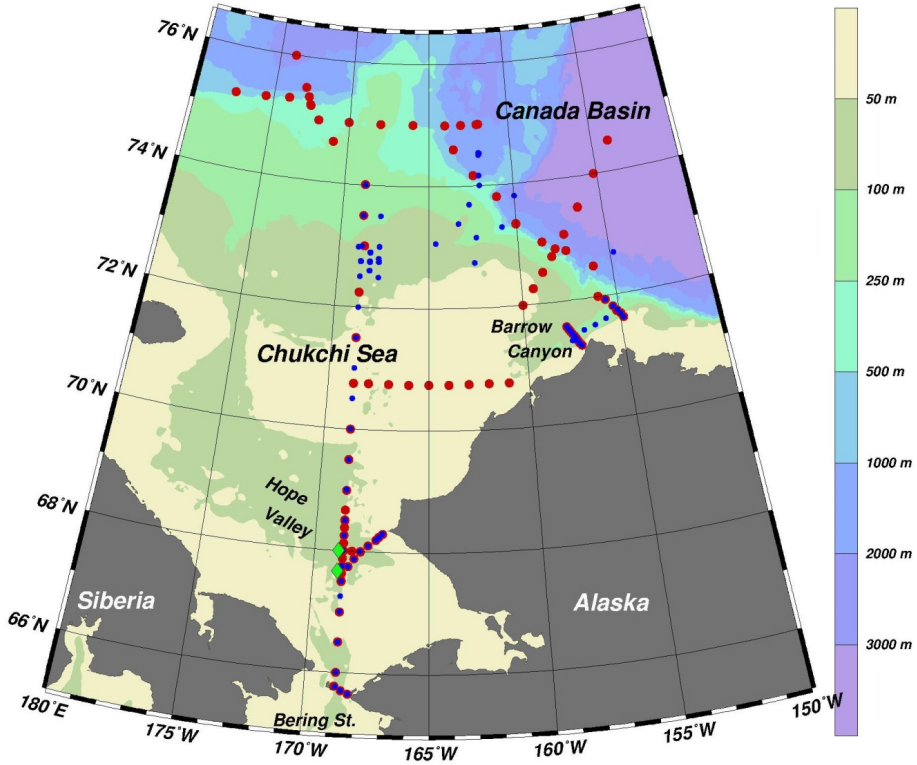

Figure 1. Map showing the bathymetric features of the study area and the hydrographic stations for the R/V *Mirai* cruises in 2012 (red dots) and 2013 (blue dots). Green diamonds represent the SCH-12 (southern site) and SCH-12-2/SCH-13 (northern site) mooring sites listed in Table 1.

BGD
12, 16359–16396, 2015

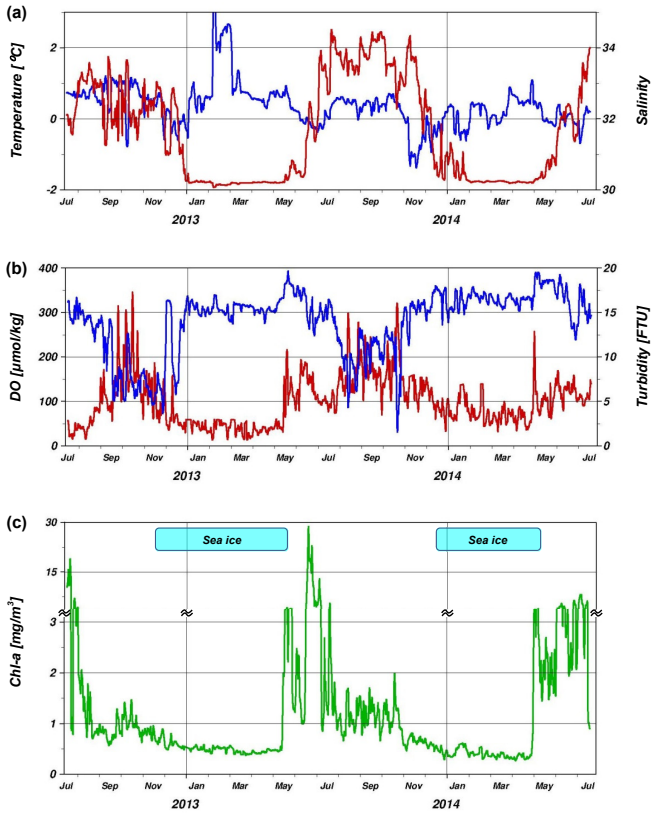

Figure 2. Time series of **(a)** temperature (°C; red) and salinity (blue), **(b)** dissolved oxygen, DO, (µmol kg^{-1}; blue) and turbidity (in formazin turbidity units, FTUs; red), and **(c)** chlorophyll *a*, Chl *a*, (mg m^{-3}; green). The data were obtained from the SCH-12, SCH-12-2, and SCH-13 moorings during 16 July 2012–19 July 2014. The vertical axis scale in **(c)** is exaggerated where the concentration is < 3 mg m^{-3}. Periods when sea ice concentration was > 50 % at the mooring site are indicated by blue bars.

BGD
12, 16359–16396, 2015

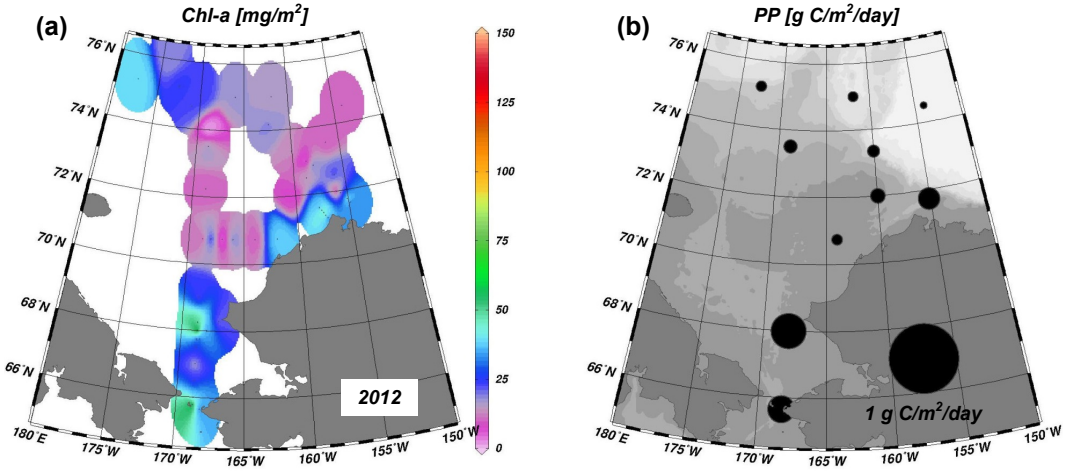

Figure 3. (a) Chlorophyll *a* integrated over the water column (mg m^{-2}) and **(b)** daily primary productivity in the water column (g C m^{-2} d^{-1}) obtained from the 2012 R/V *Mirai* cruise.

BGD
12, 16359–16396, 2015

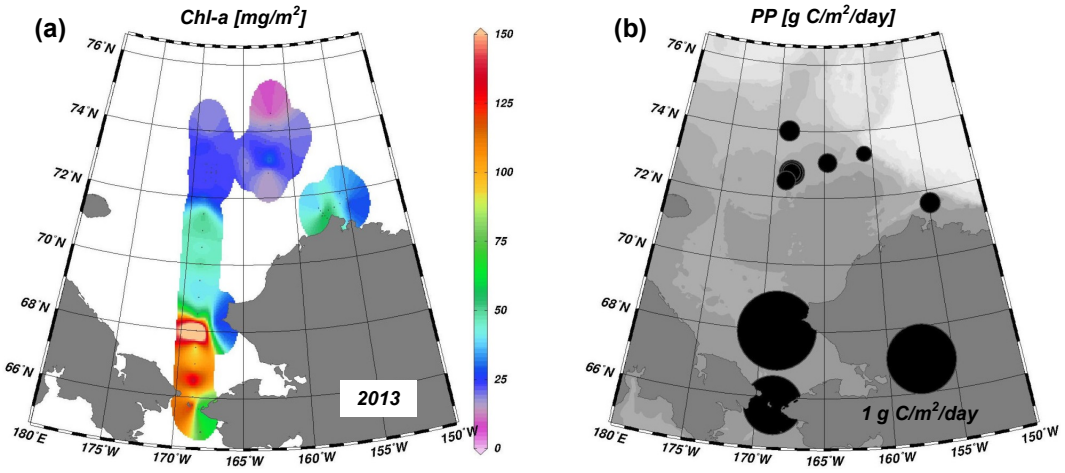

Figure 4. (a) Chlorophyll *a* integrated over the water column (mg m^{-2}) and **(b)** daily primary productivity in the water column (g C m^{-2} d^{-1}) obtained from the 2013 R/V *Mirai* cruise.

BGD
12, 16359–16396, 2015

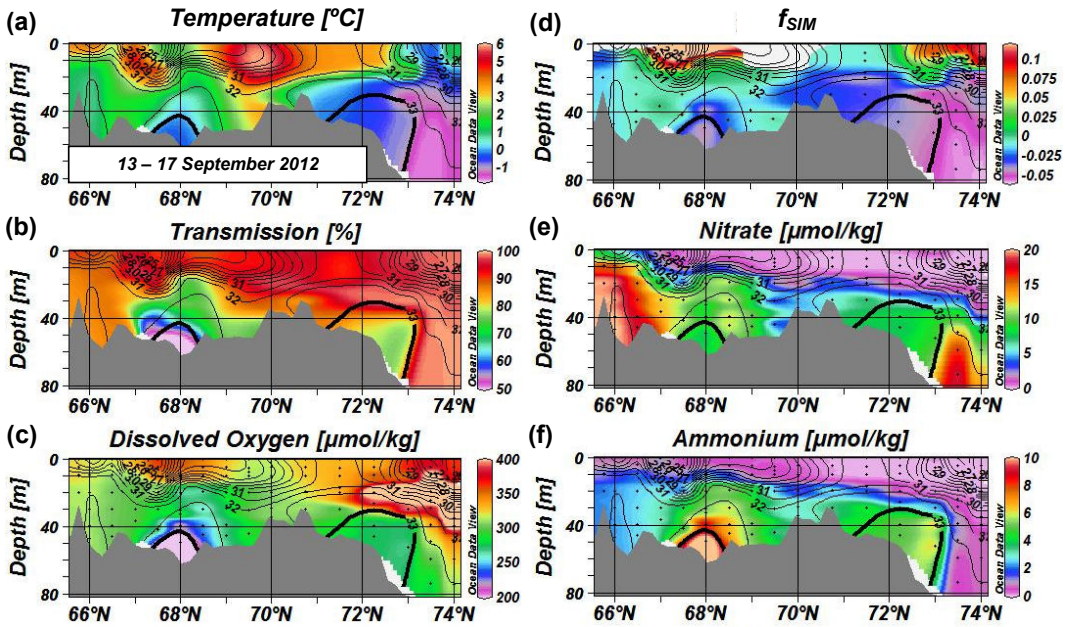

Figure 5. Vertical sections of **(a)** temperature (˚C), **(b)** light transmission (%), **(c)** dissolved oxygen (µmol kg^{-1}), **(d)** fraction of sea ice meltwater, **(e)** nitrate (µmol kg^{-1}), and **(f)** ammonium (µmol kg^{-1}) along the 168˚45′ W meridian near the US–Russia border obtained during the 13–17 September 2012 R/V *Mirai* cruise. The water sampling level at each station is indicated by a black dot. Salinity contours are superimposed on each section with a 0.5 contour interval. The thick contour in each section indicates a salinity of 33.

BGD
12, 16359–16396, 2015

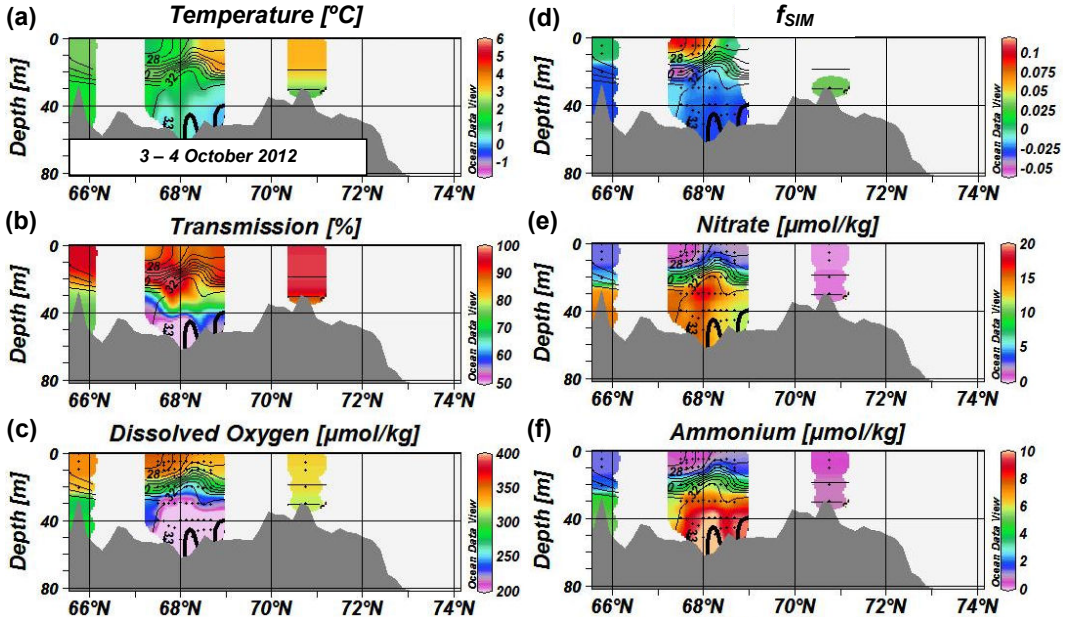

Figure 6. Vertical sections of **(a)** temperature (˚C), **(b)** light transmission (%), **(c)** dissolved oxygen (µmol kg^{-1}), **(d)** fraction of sea ice meltwater, **(e)** nitrate (µmol kg^{-1}), and **(f)** ammonium (µmol kg^{-1}) along the 168˚45′ W meridian near the US–Russia border obtained during the 3–4 October 2012 R/V *Mirai* cruise. The water sampling level at each station is indicated by a black dot. Salinity contours are superimposed on each section with a 0.5 contour interval. The thick contour in each section indicates a salinity of 33.

BGD
12, 16359–16396, 2015

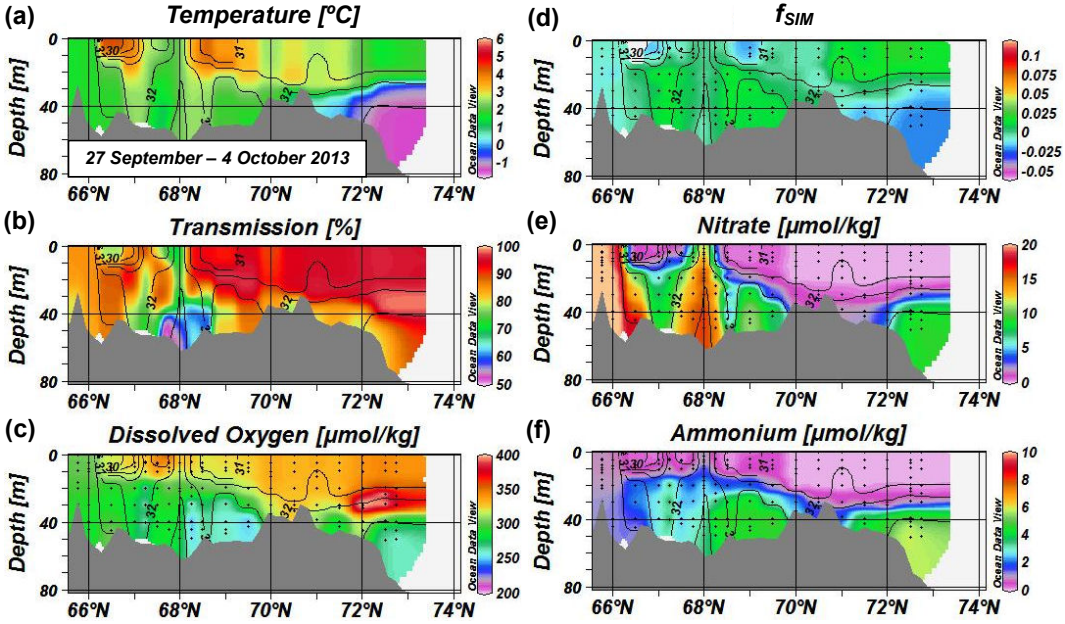

Figure 7. Vertical sections of **(a)** temperature (˚C), **(b)** light transmission (%), **(c)** dissolved oxygen (µmol kg^{-1}), **(d)** fraction of sea ice meltwater, **(e)** nitrate (µmol kg^{-1}), and **(f)** ammonium (µmol kg^{-1}) along the 168˚45′ W meridian near the US–Russia border obtained during the 27 September–4 October 2013 R/V *Mirai* cruise. The water sampling level at each station is indicated by a black dot. Salinity contours are superimposed on each section with a 0.5 contour interval.

BGD
12, 16359–16396, 2015

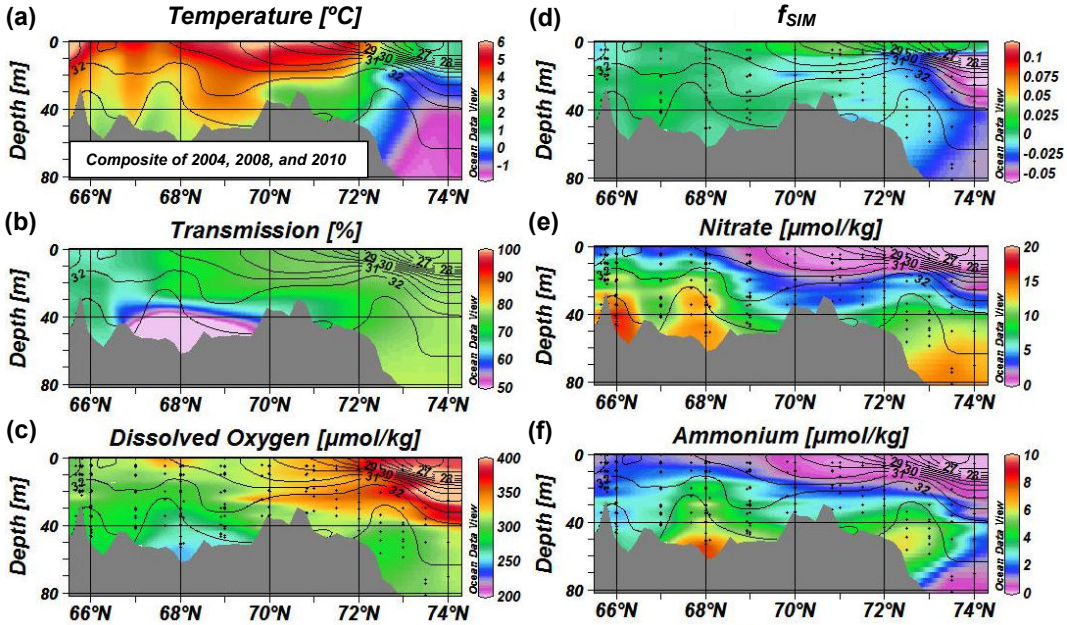

Figure 8. Vertical sections of **(a)** temperature (˚C), **(b)** light transmission (%), **(c)** dissolved oxygen (µmol kg^{-1}), **(d)** fraction of sea ice meltwater, **(e)** nitrate (µmol kg^{-1}), and **(f)** ammonium (µmol kg^{-1}) along the 168˚45′ W meridian near the US–Russia border obtained from composite data during the late summer to fall of 2004, 2008, and 2010 R/V *Mirai* cruises. In **(b)**, the data were available only for 2004, and had a negative bias of ∼20 %. The water sampling level at each station is indicated by a black dot. Salinity contours are superimposed on each section with a 0.5 contour interval.

BGD
12, 16359–16396, 2015

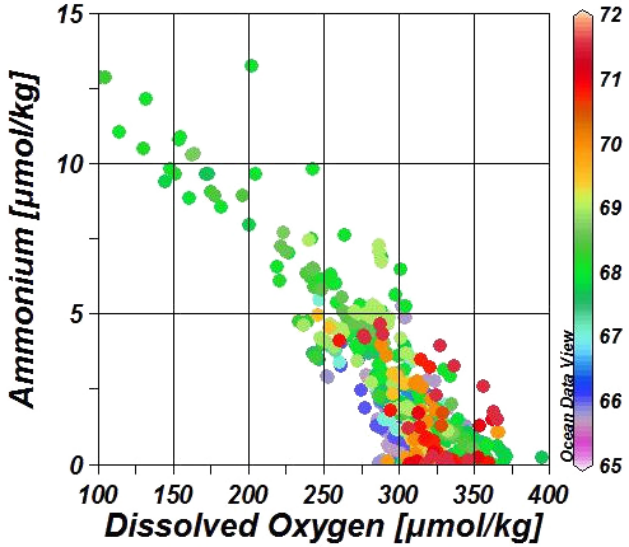

Figure 9. Diagram of dissolved oxygen (µmol kg^{-1}) and ammonium (µmol kg^{-1}) in the southern Chukchi Sea (65–72° N, 168°45′ W). Colour indicates latitude. Data were obtained from the late summer to fall 2004, 2008, 2010, 2012, and 2013 R/V *Mirai* cruises.

BGD
12, 16359–16396, 2015